Neurobiology of Disease

# Histological Underpinnings of Grey Matter Changes in Fibromyalgia Investigated Using Multimodal Brain Imaging

Florence B. Pomares,[1,2] Thomas Funck,[3] Natasha A. Feier,[1] Steven Roy,[1] Alexandre Daigle-Martel,[4] Marta Ceko,[5] Sridar Narayanan,[3] David Araujo,[3] Alexander Thiel,[6,7] Nikola Stikov,[4,8] Mary-Ann Fitzcharles,[9,10] and Petra Schweinhardt[1,2,6,11]

[1]Alan Edwards Centre for Research on Pain, McGill University, Montreal, Quebec H3A 0C7, Canada, [2]Faculty of Dentistry, McGill University, Montreal, Quebec H3A 0C7, Canada, [3]McConnell Brain Imaging Centre, Montreal Neurological Institute, McGill University, Montreal, Quebec, H3A 2B4, Canada, [4]Institute for Biomedical Engineering, École Polytechnique, Montreal, Quebec H3T 1J4, Canada, [5]Institute of Cognitive Science, University of Colorado, Boulder, Colorado 80309, [6]Department of Neurology & Neurosurgery, McGill University, Montreal, Quebec H3A 0C7, Canada, [7]Jewish General Hospital, Montreal, Quebec H3T 1E2, Canada, [8]Montreal Heart Institute, Montreal, Quebec, H1T 1C8, Canada, [9]Division of Rheumatology, McGill University Health Centre, Montreal, Quebec H3G 1A4, Canada, [10]Alan Edwards Pain Management Unit, McGill University Health Centre, Montreal, Quebec H3G 1A4, Canada, and [11]Interdisciplinary Spinal Research, Department of Chiropractic Medicine, University Hospital Balgrist, 8008 Zurich, Switzerland

Chronic pain patients present with cortical gray matter alterations, observed with anatomical magnetic resonance (MR) imaging. Reduced regional gray matter volumes are often interpreted to reflect neurodegeneration, but studies investigating the cellular origin of gray matter changes are lacking. We used multimodal imaging to compare 26 postmenopausal women with fibromyalgia with 25 healthy controls (age range: 50 –75 years) to test whether regional gray matter volume decreases in chronic pain are associated with compromised neuronal integrity. Regional gray matter decreases were largely explained by T1 relaxation times in gray matter, a surrogate measure of water content, and not to any substantial degree by $GABA_A$ receptor concentration, an indirect marker of neuronal integrity measured with [$^{18}$F] flumazenil PET. In addition, the MR spectroscopy marker of neuronal viability, $N$-acetylaspartate, did not differ between patients and controls. These findings suggest that decreased gray matter volumes are not explained by compromised neuronal integrity. Alternatively, a decrease in neuronal matter could be compensated for by an upregulation of $GABA_A$ receptors. The relation between regional gray matter and T1 relaxation times suggests decreased tissue water content underlying regional gray matter decreases. In contrast, regional gray matter increases were explained by $GABA_A$ receptor concentration in addition to T1 relaxation times, indicating perhaps increased neuronal matter or $GABA_A$ receptor upregulation and inflammatory edema. By providing information on the histological origins of cerebral gray matter alterations in fibromyalgia, this study advances the understanding of the neurobiology of chronic widespread pain.

*Key words:* chronic pain; flumazenil PET; grey matter; neurodegeneration; voxel-based morphometry

---

### Significance Statement

Regional gray matter alterations in chronic pain, as detected with voxel-based morphometry of anatomical magnetic resonance images, are commonly interpreted to reflect neurodegeneration, but this assumption has not been tested. We found decreased gray matter in fibromyalgia to be associated with T1 relaxation times, a surrogate marker of water content, but not with $GABA_A$ receptor concentration, a surrogate of neuronal integrity. In contrast, regional gray matter increases were partly explained by $GABA_A$ receptor concentration, indicating some form of neuronal plasticity. The study emphasizes that voxel-based morphometry is an exploratory measure, demonstrating the need to investigate the histological origin of gray matter alterations for every distinct clinical entity, and advances the understanding of the neurobiology of chronic (widespread) pain.

---

## Introduction

Brain atrophy occurs in a variety of different neurological and psychiatric conditions and was traditionally identified postmor-

tem. With the advent of high-resolution anatomical MRI, it has become possible to analyze gray matter volumes (GMVs) *in vivo* and to detect subtle, regionally confined decreases in cerebral

gray matter. Regional gray matter decreases have been described in patients with Alzheimer's disease, Parkinson's disease, and schizophrenia (Mueller et al., 2012a, b), among others. Chronic pain is no exception and is associated with regional GMV decreases in several cortical and subcortical areas, including the cingulate cortex, insula, prefrontal cortex, and the thalamus, as confirmed in meta-analyses (Davis and Moayedi, 2013; Smallwood et al., 2013).

Neurodegeneration, the progressive damage of neurons, is known to occur in many conditions involving brain atrophy. In Alzheimer's disease, for example, hippocampal gray matter decreases as detected with MRI were related to decreased numbers of neurons (Bobinski et al., 2000; Duyckaerts et al., 2009). Neurodegeneration provides an attractive explanation for the deleterious effects chronic pain has on cognitive and emotional processing (Bushnell et al., 2013). However, whether GMV decreases in chronic pain are associated with compromised neuronal integrity has not been tested.

In addition to regional gray matter decreases, increases are observed in chronic pain, albeit less extensively and less consistently (Davis and Moayedi, 2013; Smallwood et al., 2013). We have speculated that regional gray matter increases reflect supraspinal inflammation in chronic pain (Schweinhardt et al., 2008). Alternatively, increased gray matter in chronic pain might be caused by increased use of certain neuronal populations, akin to plastic changes in synapses and neural processes described for learning (e.g., Anderson, 2011; Draganski et al., 2011; for review, see Zatorre et al., 2012). Similar to gray matter decreases, tissue properties underlying gray matter increases in chronic pain have not been investigated.

Using multimodal imaging, we aimed to better understand the nature of cerebral gray matter alterations in fibromyalgia, in which the cardinal symptom is chronic widespread pain (Mease et al., 2009). The assessment of regional GMVs with high-resolution T1-weighted MRI, as done in previous studies, enables the investigation of subtle changes in regional GMVs; however, it cannot determine which tissue or cell types are affected. Therefore, we complemented GMV measures with [$^{18}$F]flumazenil PET, proton magnetic resonance (MR) spectroscopy, and voxel-based quantitative T1 relaxometry. Flumazenil binds to the benzodiazepine site of the $\gamma$-aminobutyric acid (GABA$_A$) receptor, which is densely expressed at inhibitory synapses in the cortex (Holthoff et al., 1991; Sette et al., 1993; Heiss et al., 1998). Because the benzodiazepine-GABA$_A$ receptor complex is located on neurons, [$^{18}$F]flumazenil PET has been used as a surrogate marker of neuronal density in gray matter (la Fougère et al., 2011) and of neuronal integrity (Heiss et al., 2001). The concentration of N-acetylaspartate, measured with proton MR spectroscopy, served as additional read-out of neuronal viability (Moffett et al., 2007). Finally, quantitative T1 relaxometry was used as a surrogate measure of tissue water content (Fatouros et al., 1991; Gelman et al., 2001) because alterations in water content might influence apparent gray matter (Lorio et al., 2016).

## Materials and Methods

### Participants

Postmenopausal women were studied because fibromyalgia predominantly affects women (Staud, 2006) and because premenopausal and

postmenopausal fibromyalgia patients have been reported to show different patterns of regional gray matter alterations (Ceko et al., 2013). The McGill Institutional Review Board approved the study, and participants gave written informed consent before inclusion. Exclusion criteria were: pain conditions other than fibromyalgia, uncontrolled medical conditions, any psychiatric or neurological disorders, and body mass index >30 kg/m$^2$. Participants using benzodiazepine medication more than once a week were excluded. Participants using benzodiazepines occasionally (4 patients once a week, 2 patients biweekly) were off medication for at least 48 h before the PET scan to avoid potential interactions of benzodiazepines with the radiotracer. Of 59 participants recruited, 8 were excluded from analysis: 4 participants had one or more missing imaging modalities, 3 had poor quality PET data, and 1 had visible atrophy. The final sample comprised 26 patients and 25 controls with complete imaging data. The healthy control group was matched to the fibromyalgia group for age, body mass index, education level, income, and physical activity level [short version of the International Physical Activity Questionnaire (Craig et al., 2003)] because these factors can influence regional GMVs. An experienced rheumatologist (M.-A.F.) confirmed the diagnosis of fibromyalgia according to the 2012 Canadian Guidelines (Fitzcharles et al., 2013), before inclusion.

Participants took part in three 1.5-h-long sessions: a psychophysical/questionnaire session, one MRI, and one PET session. Thirty-seven participants of 51 had the three sessions within a 2 week period, nine within 1 month, and four within 3 months. For one participant, the MRI session was separated from the PET and psychophysical session by 1 year because poor data quality required repeating the MRI session.

### Psychophysical/questionnaire session

Participants were asked about their current pain level and tested for pain sensitivity (pressure pain on the thumb), completed the Beck Depression Inventory (Beck et al., 1961), the Hospital Anxiety and Depression Scale (Zigmond and Snaith, 1983), the Pain Catastrophizing scale (Sullivan et al., 1995) (maximum score 52, clinically relevant score >30), and the Fibromyalgia Impact Questionnaire (Bennett, 2005). Participants were also assessed using the Attention Network Test (Fan et al., 2002) and the Auditory Consonant Trigram test (Stuss et al., 1988). The data from the pain testing as well as the cognitive testing are not included in this report.

### Image acquisition

*MRI and spectroscopy.* MRI was performed using a 3 tesla Tim Trio Siemens scanner (Siemens Medical Solutions) with a 12-channel head coil. Three types of data were acquired: anatomical T1-weighted images to assess regional GMVs, absolute T1 relaxation times to assess water content, and proton MR spectroscopy to measure metabolite levels, specifically N-acetylaspartate (NAA) and N-acetylaspartyl-glutamate (NAAG).

For T1-weighted images, a 3D MP-RAGE sequence with the following parameters was used: repetition time 2300 ms, echo time 2.98 ms, flip angle 9°, field of view 256 mm, 192 slices in the sagittal plane, resolution $1 \times 1 \times 1$ mm; acquisition time 10 min.

To compute maps of absolute T1 relaxation times, T1 mapping was performed using Variable Flip Angle mapping (Deoni et al., 2005) with the following parameters: repetition time 15 ms, echo time 3.21 ms, flip angle 3° and 20°, field of view 256 mm, 160 slices, resolution $1 \times 1 \times 1$ mm. The Actual Flip Angle sequence (Yarnykh, 2007) was used to correct for inhomogeneities of the radiofrequency magnetic field (B1), with the following parameters: repetition time 20 ms, $N = 5$, echo time 3.53 ms, flip angle 60°, field of view 256 mm, 44 slices, slice thickness 4 mm, in-plane resolution $2 \times 2$ mm; acquisition time 19 min.

Single-voxel proton MR spectroscopy was performed using a Point Resolved Spectroscopy sequence (Bottomley, 1984) with the following parameters: repetition time 3000 ms, echo time 30 ms, 196 acquisitions; acquisition time 10 min. A $20 \times 40 \times 15$ mm voxel was positioned in the anterior cingulate cortex (ACC) (Fig. 1) because it consistently displays GMV decreases in chronic pain including fibromyalgia (Smallwood et al., 2013), plays an important role in pain processing, and is more suitable for MR spectroscopy compared with some other brain regions because of the relative lack of susceptibility artifacts and signal inhomogeneities.

*PET.* Data were acquired using an ECAT High-Resolution Research Tomograph (Siemens Medical Solutions), which has a spatial resolution of 2.3–3.4 mm at FWHM. The radiopharmaceutical [$^{18}$F]flumazenil was synthesized as published previously (Massaweh et al., 2009). After a transmission scan for attenuation correction ($^{137}$Cs-source), ~370 MBq of [$^{18}$F]flumazenil was injected intravenously as a slow bolus over 60 s. List-mode data were acquired for 60 min after injection and were subsequently binned into fully 3D sinograms for a total of 17 time frames (40, 20, 2 × 30, 3 × 60, 4 × 150, 3 × 300, and 3 × 600 s).

### Image analysis
Data were analyzed in a blinded fashion with any group identifying information (patient or control) removed. The quality of the raw data from each imaging modality as well as at each processing step in each modality's processing pipeline was carefully checked.

### Voxel-based morphometry (VBM)
Regional GMVs were obtained by VBM analysis (Ashburner and Friston, 2000) using the VBM8 toolbox (RRID:SCR_014196) in the Statistical Parametric Mapping software (SPM8 revision 4667, Wellcome Trust Centre for Neuroimaging, RRID:SCR_007037) on the anatomical T1-weighted images. The following analysis steps were performed: (1) Image normalization to the MNI standard space using linear and nonlinear transformations (sixth generation nonlinear International Consortium for Brain Mapping template) and tissue probability maps. (2) Segmentation of the normalized images into gray matter, white matter, and CSF using the intensity distribution of the images. (3) Modulation of the gray matter segments (i.e., the intensity of each voxel was multiplied by the amount of contraction or expansion estimated by the nonlinear transformation to obtain relative volumes corrected for brain size and gross anatomical differences). (4) The modulated normalized gray matter segments were spatially blurred with a 7 × 7 × 7 mm (FWHM) Gaussian smoothing kernel (Fig. 2).

### Voxel-based relaxometry (VBR)
To compute T1 maps, the B1 maps were used to correct transmit field inhomogeneities, ensuring that the flip angles in the Variable Flip Angle acquisitions are accurate across the field of view. The two corrected Variable Flip Angle images were used to infer absolute T1 relaxation times (Deoni et al., 2005), which are independent of the acquisition parameters and comparable between different scanners and sites (Cheng et al., 2012). The resulting maps, which reflect extracellular and intracellular water (Cheng et al., 2012), were masked for the head. To analyze T1 relaxation times on a voxelwise basis, we developed an analysis pipeline specific for this purpose: (1) Each participant's voxelwise map of T1 relaxation time was registered to the corresponding T1-weighted image. (2) The nonsmoothed gray matter segment output from VBM8 was thresholded to keep only voxels containing at least 90% of gray matter, then binarized. (3) The binarized gray matter segment was used to mask the T1 maps. (4) To spatially normalize the T1 maps, the transformation matrix (from native T1-weighted image space to standard MNI space) was applied to the masked map of T1 relaxation times. The T1 maps were not modulated (not multiplied by the amount of contraction or expansion estimated by the nonlinear transformation) to preserve the quantitative information. (5) The resulting T1 maps in gray matter were spatially blurred with a 7 × 7 × 7 mm (FWHM) Gaussian smoothing kernel (Fig. 2).

To test the validity of the measurements, we added an alternative analysis to infer water content based on proton density (PD) measurements, obtained from the same T1 mapping protocol. To circumvent problems associated with high correlations between T1 and PD (Fatouros et al., 1991), the PD maps were normalized by the average PD in CSF,
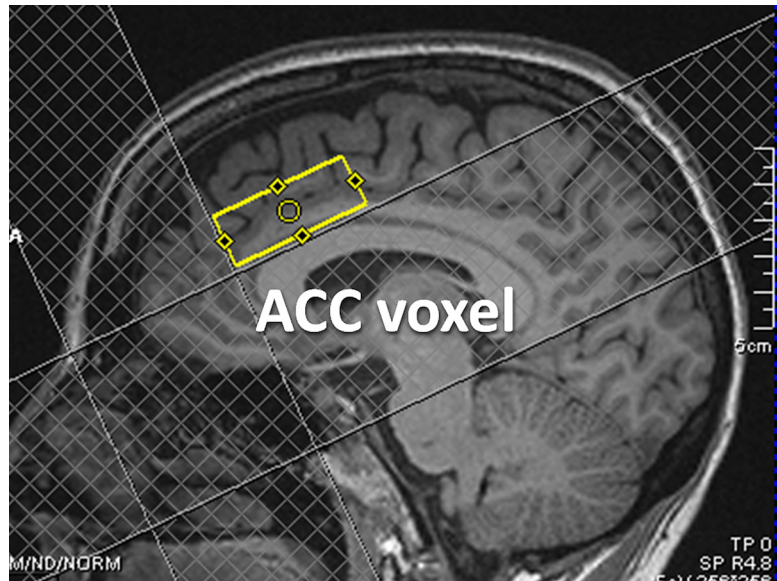


**Figure 1.** Proton MR spectroscopy voxel. Localization of the 20 × 40 × 15 mm voxel in the ACC for MR spectroscopy in a single subject.

as per Mezer et al. (2013). Thereby, the resulting water volume fraction (WVF) maps ($WVF_{voxel} = PD_{voxel}/PD_{CSF}$) are highly reproducible across subjects and field strengths (Mezer et al., 2013). The remaining processing steps (coregistration with the T1-weighted scan, masking of the gray matter, application of transformations to standard space, and smoothing) were identical to the analysis of T1 relaxation times.

### Proton MR spectroscopy
Postprocessing of the spectroscopy data was performed using LC Model (Provencher, 1993) (RRID:SCR_014455), which explicitly fits the baseline, thereby achieving high sensitivity. LC Model is an operator-independent software that fits *in vivo* metabolite spectra by using model spectra previously acquired from similar scanning conditions from various compounds in phantom solutions. Concentration ratios relative to Creatine (Cr) were computed for NAA + NAAG (denoted tNA). In mature brain, NAA and NAAG are present exclusively in neurons and their processes, and thus serve as markers of neuronal viability (Moffett et al., 1991). Given that the NAAG resonance is much smaller than that of NAA, and there is considerable overlap, the total signal is more robustly quantified. Quality control criteria for retaining spectra included Cramer-Rao SD of the total *N*-acetyl group fit <10% (mean ± SD: 3 ± 0.8%), peak FWHM <0.08 ppM, spectrum signal-to-noise ratio >10 (mean ± SD: 37 ± 7), and low residual spectrum. GMV, nondisplaceable binding potential ($BP_{ND}$), and water content were extracted from the spectroscopy voxel volume in native space. The MR spectroscopy voxel masks were created from information in the raw spectroscopy data.

### PET
We computed the $BP_{ND}$ maps from the PET images. $BP_{ND}$ of a reversibly binding radioligand is related to the maximum available concentration of its receptor ($B_{max}$) accounting for the binding affinity of the tracer (A) and the fraction ($f_{ND}$) of nondisplaceable tracer bound (i.e., tracer irreversibly bound to other molecules than the receptor) in the tissue ($BP_{ND} = f_{ND} × B_{max} × A$). Thus, $BP_{ND}$ of flumazenil represents the signal in the brain arising from the fraction of radiotracer that is specifically bound to the benzodiazepine site of GABA$_A$ receptors. Lower flumazenil $BP_{ND}$ indicates a lower concentration of GABA$_A$ receptors, which could be caused by receptor downregulation, decreased neuronal matter, or compromised neuronal integrity (Heiss et al., 2001).

Raw PET images were reconstructed by fully 3D filtered backprojection by a 3D reprojection method and corrected for participants' head motion. The $BP_{ND}$ maps were computed with the "iterative deconvolution with surface-based anatomically constrained filtering"
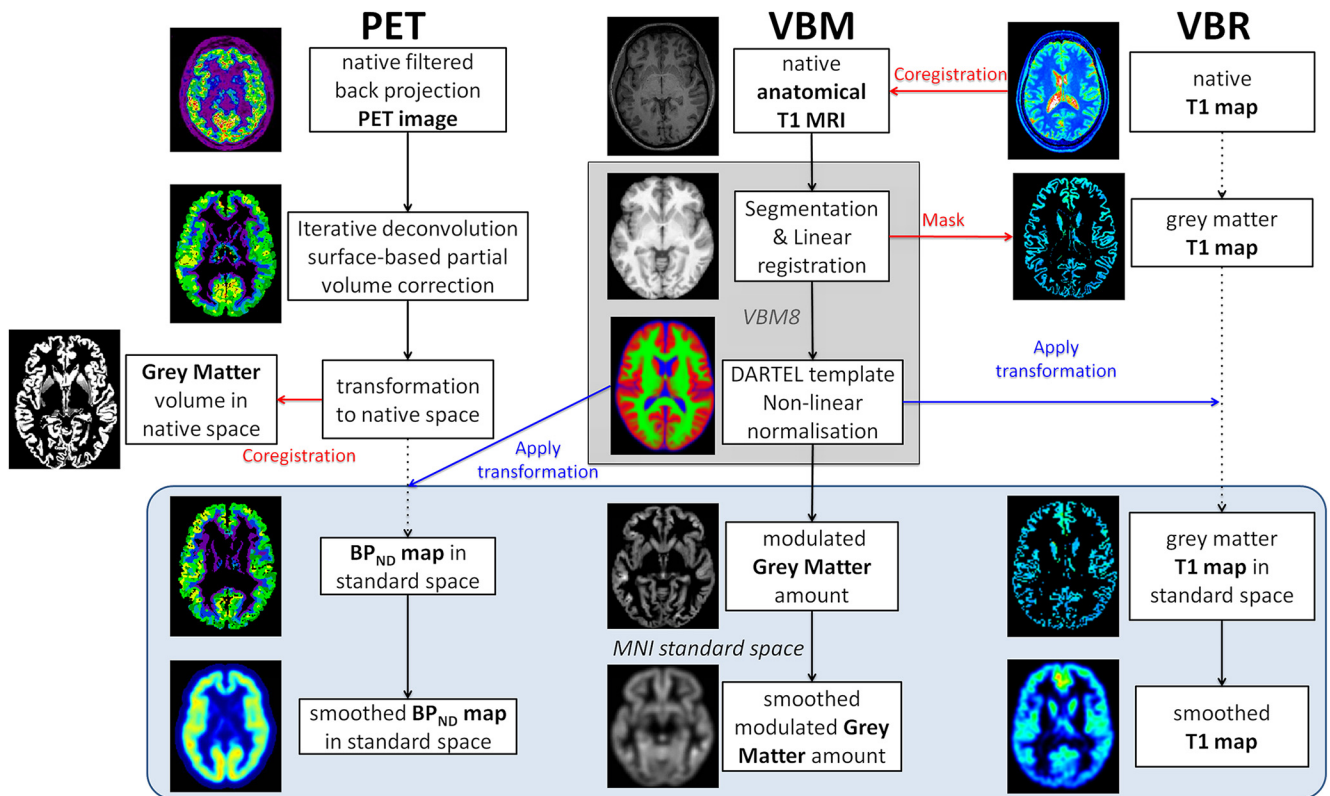
**Figure 2.** Processing pipelines. Middle, VBM analysis of GMVs. Other panels, Voxel-based analysis pipelines that we developed specifically for analysis of $BP_{ND}$ maps for flumazenil PET (left), and voxel-based relaxometry (VBR) analysis of T1 maps, a surrogate marker of water content (right). Blue box represents data in standard space (MNI space).

(idSURF) method as published by Funck et al. (2014). The idSURF algorithm corrects for partial volume effects and reconstructs a high-resolution signal in the cortical gray matter in MNI standard space. (1) The idSURF algorithm uses the representation of the volume above the white matter-gray matter surface and below the gray matter-CSF surface as a spatial constraint to the PET signal. (2) To estimate $BP_{ND}$, the Logan plot is applied to the high-resolution data using the white matter segments as low receptor density reference region because there are no benzodiazepine-$GABA_A$ receptor complexes on myelinated axons (Hammers et al., 2003). The white matter segments were eroded to limit radioactivity spill over from adjacent gray matter. (3) $BP_{ND}$ maps were back-transformed to native MRI space, and the VBM8 transformation was applied to the data. (4) Resulting $BP_{ND}$ maps in gray matter were spatially blurred with a $7 \times 7 \times 7$ mm FWHM Gaussian smoothing kernel (Fig. 2).

*Statistical analysis*
*Group differences between fibromyalgia patients and healthy controls.* Clinical variables and questionnaire data were compared between groups using two-sample two-sided Student's $t$ tests in SPSS (version 17.0, RRID:SCR_002865). The tNA/Cr ratio in the ACC was compared between groups using a univariate GLM with the percentage of gray matter in the spectroscopy voxel and/or age as covariates of no interest.

Statistical analysis of VBM was performed in SPM8 with nonuniformity smoothness correction (Worsley et al., 1999). A GLM was used for GMV analysis to compare patients and controls with age as a covariate of no interest. Two approaches were used for statistical inference: (1) a voxel-based threshold of $Z > 2.3$ (corresponding to a $p < 0.01$) corrected for spatial extent across the whole brain using cluster-level correction based on random field theory at $p < 0.05$ (Worsley et al., 2004); and (2) a voxel-based threshold of $Z > 2.3$ combined with a more lenient extent threshold of $k > 200$ contiguous voxels to reduce the probability of a Type II statistical error.

**Table 1. Participants' demographic and clinical data[a]**

| | Patients | | Controls | | Group |
|---|---|---|---|---|---|
| | Mean | SD | Mean | SD | difference ($p$) |
| Age (yr) | 61 | 5.4 | 61 | 7.6 | 0.86 |
| BMI (kg/m$^2$) | 26 | 3.7 | 25 | 3.9 | 0.27 |
| Education (yr) | 15 | 4.1 | 16 | 4.0 | 0.18 |
| Income (in 1000$/year) | 44 | 24 | 40 | 28 | 0.62 |
| IPAQ score (MET, minutes/week)[b] | 2831 | 3717 | 2735 | 2912 | 0.92 |
| GMV (ml) | 595 | 42 | 578 | 32 | 0.12 |
| White matter volume (ml) | 481 | 56 | 467 | 38 | 0.29 |
| CSF (ml) | 230 | 37 | 227 | 34 | 0.76 |
| Total volume (ml) | 1307 | 100 | 1273 | 82 | 0.19 |
| Time since diagnosis (yr) | 9 | 8 | NA | NA | |
| Symptom duration (yr) | 16 | 9 | NA | NA | |
| Current pain level (1–10) | 4.8 | 2.2 | 0.7 | 1 | <0.001 |
| BDI score (1–63) | 16 | 10 | 4 | 4 | <0.001 |
| HADS score (1–42) | 16 | 6 | 6 | 4 | <0.001 |
| PCS score (1–52) | 22 | 13 | 7 | 9 | <0.001 |
| FIQ score (1–100) | 51 | 18 | 7 | 8 | <0.001 |

[a]BMI, Body mass index; IPAQ, International Physical Activity Questionnaire; BDI, Beck Depression Inventory; HADS, Hospital Anxiety and Depression Scale; FIQ, Fibromyalgia Impact Questionnaire; PCS, Pain Catastrophizing Scale; NA, not applicable. Brain volumes were derived from native space. Total volume refers to gray matter + white matter + CSF. FIQ is based on questions, such as "Were you able to do laundry with a washer and dryer (in the past week)?" Therefore, the FIQ can be completed by control participants.

[b]MET, Metabolic equivalent intensity levels (median); 1 MET is considered a resting metabolic rate obtained during quiet sitting. Participants were on average minimally active.

*Contribution of $BP_{ND}$ and water content to GMV*
Areas showing GMVs differences between patients and controls were used as regions of interest (ROIs) in which flumazenil $BP_{ND}$ and water content were investigated. Hierarchical multiple regression analyses were used to test whether $BP_{ND}$, water content, and group (patients or controls), in this order, significantly contributed to GMV. Visual inspection of scatter plots indicated that the assumptions of linearity were met. The studentized residuals were normally distributed and homoscedastic. We
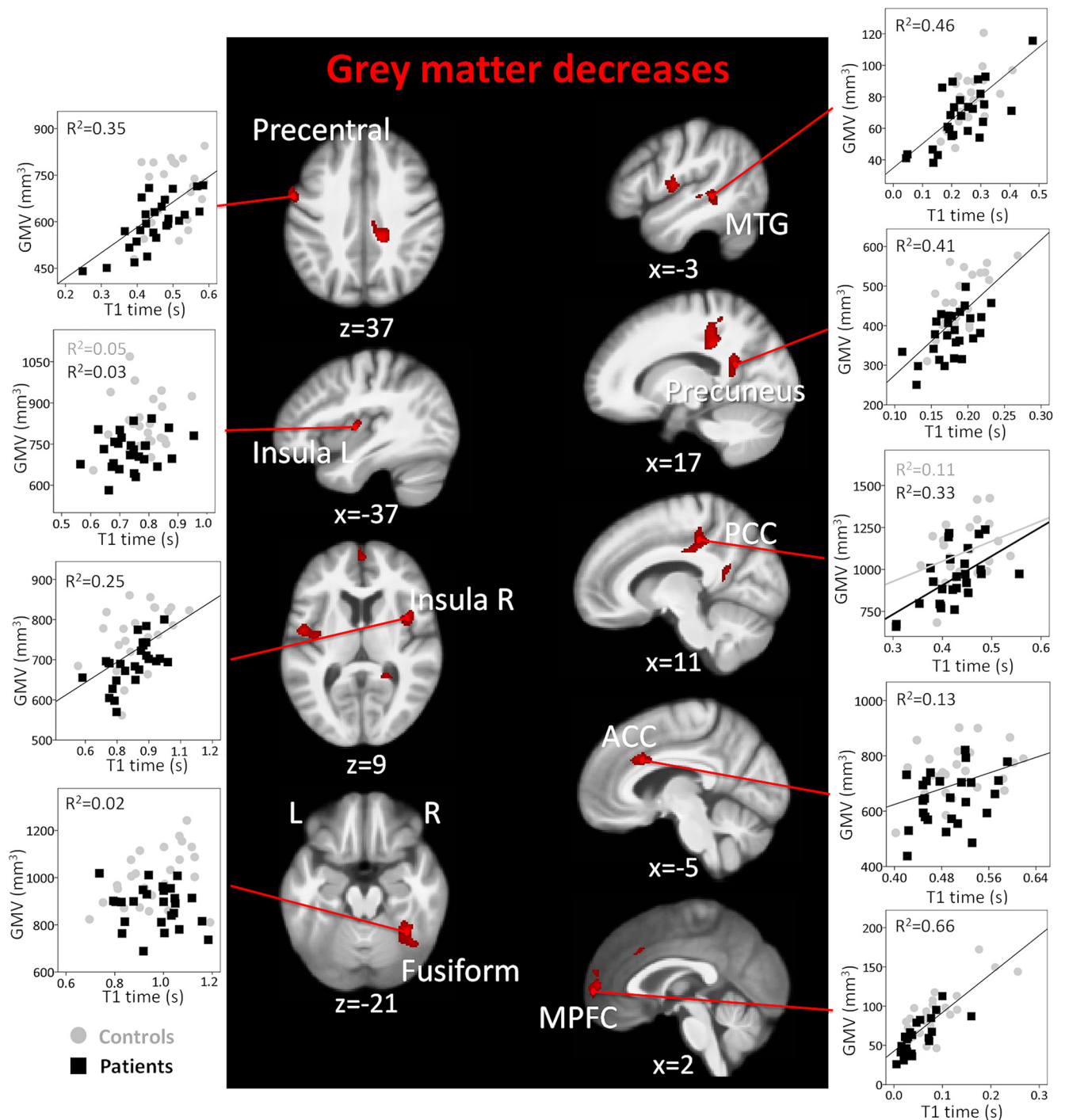
## Grey matter decreases

Precentral

$R^2=0.35$

Insula L

$R^2=0.05$
$R^2=0.03$

$R^2=0.25$

$R^2=0.02$

z=37

x=-37

z=9

z=-21

L　R

Fusiform

● Controls
■ Patients

MTG

x=-3

Precuneus

x=17

PCC

x=11

ACC

x=-5

MPFC

x=2

$R^2=0.46$

$R^2=0.41$

$R^2=0.11$
$R^2=0.33$

$R^2=0.13$

$R^2=0.66$

**Figure 3.** GMV decreases in patients with fibromyalgia and their relationship with tissue water content. Whole-brain map of GMV decreases in patients compared with controls. Results are presented at a voxelwise threshold of $z > 2.3$ and a cluster-extent threshold of $k > 200$, overlaid on the mean anatomical image of the whole sample ($N = 51$). Scatter plots represent GMV (in mm$^3$) and T1 time in seconds (a surrogate for water content) in each significant cluster. Axial images are displayed in neurological convention. Right, Right hemisphere.

included interaction terms between $BP_{ND}$ and group as well as water content and group to assess the influence of group on the relationship between gray matter and $BP_{ND}$ or water content. The mean values of modulated gray matter density, $BP_{ND}$, and water content within the ROIs in standard space were extracted in MATLAB 8.1 (The MathWorks, RRID:SCR_001622) using the spm_summarise SPM8 function. The modulated gray matter density in each ROI was transformed to volume by taking into account voxel size as in Kurth et al. (2015). GMV (in mm$^3$) served as the dependent variable; $BP_{ND}$ (unitless), water content (T1 relaxation times in seconds, the longer T1, the more water in the tissue), group, and the interaction terms served as the explanatory variables.

Finally, the effect size and power of the $BP_{ND}$ difference between groups were calculated for each ROI.

*Correlation with clinical variables*
Pearson's correlation analyses (one-tailed) were performed to assess the clinical significance of the GMV changes in patients. We tested whether GMVs in areas of decreased gray matter were negatively correlated with questionnaire scores (Fibromyalgia Impact Questionnaire, Hospital Anxiety and Depression Scale, Beck Depression Inventory, Pain Catastrophizing Scale), current pain level, time since diagnosis, and symptom duration. Inversely, we tested whether GMVs in areas of gray matter

increases were positively correlated with clinical variables. Correlation analyses were considered exploratory and therefore nor corrected for multiple comparisons.

*Replication of PET and VBM relationship*
To test whether we could replicate a previously reported relationship between PET and VBM measures, we tested our healthy control group for the significant positive correlations between gray matter density and flumazenil $BP_{ND}$ described by Duncan et al. (2013) for young healthy adults. We followed their approach and conducted weighted least square regression analyses between gray matter density and $BP_{ND}$ in regions defined by the Jülich histological atlas (Eickhoff et al., 2006, 2007). The weighting was computed as the inverse of the variance of the $BP_{ND}$ measure within each anatomical region, for each subject.

# Results

## Participant characteristics
Patients had on average moderate pain at the time of the psycho-physical/questionnaire session (mean ± SD: 4.8 ± 2.2 on an 11-point numerical rating scale) and a moderate impact of fibromyalgia on functioning as measured by the Fibromyalgia Impact Questionnaire. Patients and controls did not differ significantly with respect to age, body mass index, education level, income, or physical activity levels. Despite having statistically higher scores on the Beck Depression Inventory, the Hospital Anxiety and Depression Scale and the Pain Catastrophizing Scale, none of the patients had clinically significant levels of depression, anxiety, or pain catastrophizing as determined by questionnaire cutoffs. Total brain volume and volumes of gray matter, white matter, and CSF were not significantly different in patients compared with healthy controls (Table 1).

## GMV decreases in patients compared with controls
In line with previous studies, fibromyalgia patients presented GMV alterations in several cortical regions. Regional GMV was decreased in patients compared with healthy controls in the posterior cingulate cortex (PCC) and precuneus, significantly when corrected for cluster extent on a whole-brain level. ACC, bilateral insula, right medial prefrontal cortex (MPFC), left precentral gyrus, left middle temporal gyrus (MTG), and right fusiform gyrus showed decreased GMV at the more lenient statistical threshold of 200 contiguous voxels (Fig. 3; Table 2).

In most regions of decreased GMV, T1 relaxation times (a surrogate measure of water content) and group (patient or control) accounted for a large proportion of the variance, with no significant contribution of flumazenil $BP_{ND}$, measuring $GABA_A$ receptor concentration (Fig. 3). T1 relaxation time accounted for between 13% (ACC) and 55% (MPFC) of the variance; only in the fusiform gyrus did T1 relaxation time not contribute significantly to the hierarchical multiple regression model. Only in the left insula, MPFC, and MTG did $GABA_A$ receptor concentration explain some gray matter variance (11%, 12%, and 12%, respectively). Closer inspection revealed a negative relationship in the left insula: the less GMV, the higher the concentration of $GABA_A$ receptors. In the precuneus, group influenced the relationship between $GABA_A$ receptor concentration and GMV: patients showed a significant positive relationship between $GABA_A$ receptor concentration and GMV, which was absent in the controls.

The results in regions of decreased GMV were largely unchanged when T1 relaxation time was entered first in the regression model. The results were very similar when using the proton density derived metric (Mezer et al., 2013) instead of T1 relaxation times as a measure of water content. Detailed results of the

**Table 2. VBM analysis results**[a]

| Region | Cluster corrected $p$ | Cluster extent (no. of voxels) | Z score | Coordinates (mm) x | y | z |
|---|---|---|---|---|---|---|
| *Gray matter decreases in patients compared with controls* | | | | | | |
| PCC R | 0.011[b] | 830 | 3.82 | 15 | −34 | 34 |
| | | | 2.98 | 10 | −24 | 33 |
| | | | 2.66 | 16 | −40 | 55 |
| Fusiform gyrus R | 0.087 | 644 | 3.66 | 36 | −49 | −21 |
| | | | 3.29 | 39 | −60 | −15 |
| | | | 2.49 | 27 | −60 | −17 |
| Insula L | 0.126 | 383 | 3.4 | −48 | −6 | 9 |
| | | | 2.79 | −39 | −10 | 7 |
| Insula R | 0.133 | 349 | 3.21 | 42 | 8 | 10 |
| MPFC R | 0.096 | 225 | 3.2 | 2 | 56 | 6 |
| | | | 2.73 | −2 | 64 | 10 |
| | | | 2.66 | 0 | 60 | −5 |
| ACC L | 0.067 | 537 | 3.19 | −3 | 23 | 30 |
| | | | 2.99 | −14 | 18 | 25 |
| | | | 2.36 | −15 | 3 | 30 |
| Precuneus R | 0.022[b] | 651 | 3.14 | 16 | −51 | 24 |
| | | | 2.94 | 33 | −48 | 0 |
| | | | 2.72 | 21 | −49 | 13 |
| Precentral gyrus L | 0.207 | 448 | 3.04 | −58 | −3 | 37 |
| | | | 2.6 | −56 | 5 | 21 |
| MTG L | 0.154 | 282 | 3.03 | −44 | −37 | 3 |
| | | | 2.8 | −46 | −40 | −6 |
| | | | 2.77 | −44 | −28 | −2 |
| *Gray matter increases in patients compared with controls* | | | | | | |
| Angular gyrus L | 0.05 | 594 | 3.83 | −39 | −60 | 40 |
| | | | 2.68 | −33 | −63 | 55 |
| Cuneus R | 0.113 | 234 | 3.38 | 12 | −81 | 46 |
| | | | 3.27 | 6 | −76 | 39 |
| Postcentral gyrus R | 0.262 | 306 | 3 | 40 | −25 | 34 |
| | | | 2.97 | 36 | −31 | 46 |
| | | | 2.37 | 39 | −27 | 56 |

[a]Whole-brain results are presented at a voxel-wise threshold of $Z > 2.3$ and cluster extent of $k > 200$ contiguous voxels. L, Left; R, right.

[b]Significant with cluster-level correction across the whole brain at $p < 0.05$.

regression analysis are found in Table 3. The finding that $GABA_A$ receptor concentration did not contribute to the gray matter variance in regions of decreased gray matter in patients is corroborated by the observation that $GABA_A$ receptor concentration was not lower in patients than in controls in any of the ROIs (highest effect size = 0.12, power = 0.07).

GMV in the ACC spectroscopy voxel was not significantly different in patients compared with controls (patients mean ± SD: 6727 ± 458 mm$^3$, controls: 6842 ± 609 mm$^3$, $F = 0.54$, $p = 0.465$) or when controlling for age. tNA/Cr ratios were in line with literature values: 1.12 ± 0.11 for patients and 1.11 ± 0.11 for controls (Nordahl et al., 2002). There was no group difference for tNA/Cr ratios when controlling for gray matter amount in the voxel, for age, or for both, indicating that neuronal viability was not affected in the ACC of the patients. There was no correlation between tNA/Cr ratios and $GABA_A$ receptor concentration in the spectroscopy voxel across the two groups ($r = −0.14$, $p = 0.314$).

## GMV increases in patients compared with controls
In line with the literature, increases of GMVs in fibromyalgia patients were less pronounced than decreases. Increased GMVs were found in the angular gyrus, cuneus, and right postcentral gyrus (Fig. 4; Table 2). In contrast to regions with GMV decreases, $GABA_A$ receptor concentration explained more variance than tissue water content. Specifically, $GABA_A$ receptor concentration explained 32% of the variance in the angular gyrus, 70% in the cuneus, and 22% in the postcentral gyrus; tissue water

**Table 3. Multiple regression results[a]**

| | Water content | | | | Proton density | | | |
|---|---|---|---|---|---|---|---|---|
| | Adjusted $R^2$ | $R^2$ change | F | p | Adjusted $R^2$ | $R^2$ change | F | p |
| **Gray matter decreases in patients compared with control** | | | | | | | | |
| PCC R | | | | | | | | |
| $BP_{ND}$ | 0.35 | 0.06 | 3.2 | 0.082 | 0.53 | 0.06 | 3.2 | 0.082 |
| T1/PD | | 0.20[b] | 12.7[b] | 0.001[b] | | 0.40[b] | 35.5[b] | <0.001[b] |
| Group | | 0.12[b] | 9.2[b] | 0.004[b] | | 0.08[b] | 8.3[b] | 0.006[b] |
| Group × $BP_{ND}$ | | 0.04 | 2.8 | 0.102 | | 0.04 | 3.9 | 0.055 |
| Group × T1/PD | | 0.00 | 0.1 | 0.730 | | 0.00 | 0.0 | 0.961 |
| Fusiform R | | | | | | | | |
| $BP_{ND}$ | | 0.01 | 0.4 | 0.509 | 0.33 | 0.01 | 0.4 | 0.509 |
| T1/PD | | 0.01 | 0.6 | 0.452 | | 0.04 | 2.1 | 0.158 |
| Group | | 0.31[b] | 21.2[b] | <0.001[b] | | 0.30 | 21.2[b] | <0.001[b] |
| Group × $BP_{ND}$ | | 0.02 | 1.4 | 0.249 | | 0.02 | 1.3 | 0.253 |
| Group × T1/PD | | 0.05 | 3.8 | 0.058 | | 0.03 | 2.2 | 0.141 |
| Insula L | | | | | | | | |
| $BP_{ND}$ | 0.31 | 0.11[b] | 5.9[b] | 0.018[b] | 0.38 | 0.11[b] | 5.9[b] | 0.018[b] |
| T1/PD | | 0.15[b] | 9.8[b] | 0.003[b] | | 0.23[b] | 16.6[b] | <0.001[b] |
| Group | | 0.11[b] | 8.1[b] | 0.007[b] | | 0.08[b] | 6.1[b] | 0.017[b] |
| Group × $BP_{ND}$ | | 0.01 | 0.4 | 0.515 | | 0.00 | 0.3 | 0.585 |
| Group × T1/PD | | 0.00 | 0.1 | 0.820 | | 0.02 | 2.0 | 0.168 |
| Insula R | | | | | | | | |
| $BP_{ND}$ | 0.34 | 0.06 | 3.4 | 0.072 | 0.42 | 0.06 | 3.4 | 0.072 |
| T1/PD | | 0.23[b] | 15.3[b] | <0.001[b] | | 0.29[b] | 21.8[b] | <0.001[b] |
| Group | | 0.11[b] | 8.9[b] | 0.005[b] | | 0.10[b] | 8.3[b] | 0.006[b] |
| Group × $BP_{ND}$ | | 0.00 | 0.1 | 0.702 | | 0.01 | 1.1 | 0.298 |
| Group × T1/PD | | 0.00 | 0.1 | 0.786 | | 0.01 | 0.8 | 0.377 |
| MPFC R | | | | | | | | |
| $BP_{ND}$ | 0.68 | 0.12[b] | 6.6[b] | 0.013[b] | 0.77 | 0.12[b] | 6.6[b] | 0.013[b] |
| T1/PD | | 0.55[b] | 79.3[b] | <0.001[b] | | 0.65[b] | 131.1[b] | <0.001[b] |
| Group | | 0.04[b] | 6.5[b] | 0.014[b] | | 0.03[b] | 6.2[b] | 0.016[b] |
| Group × $BP_{ND}$ | | 0.01 | 1.0 | 0.326 | | 0.00 | 0.3 | 0.578 |
| Group × T1/PD | | 0.00 | 0.3 | 0.594 | | 0.00 | 0.9 | 0.347 |
| ACC L | | | | | | | | |
| $BP_{ND}$ | 0.29 | 0.00 | 0.0 | 0.930 | 0.32 | 0.00 | 0.0 | 0.930 |
| T1/PD | | 0.13[b] | 6.9[b] | 0.012[b] | | 0.20[b] | 11.8[b] | 0.001[b] |
| Group | | 0.21[b] | 14.6[b] | <0.001[b] | | 0.16[b] | 11.9[b] | 0.001[b] |
| Group × $BP_{ND}$ | | 0.02 | 1.6 | 0.206 | | 0.03 | 1.9 | 0.180 |
| Group × T1/PD | | 0.00 | 0.0 | 0.861 | | 0.00 | 0.2 | 0.695 |
| Precuneus R | | | | | | | | |
| $BP_{ND}$ | 0.62 | 0.02 | 0.8 | 0.376 | 0.59 | 0.02 | 0.8 | 0.376 |
| T1/PD | | 0.42[b] | 35.1[b] | <0.001[b] | | 0.41[b] | 34.0[b] | <0.001[b] |
| Group | | 0.15[b] | 17.3[b] | <0.001[b] | | 0.15[b] | 16.8[b] | <0.001[b] |
| Group × $BP_{ND}$ | | 0.06[b] | 7.3[b] | 0.010[b] | | 0.05[b] | 5.8[b] | 0.020[b] |
| Group × T1/PD | | 0.02 | 2.0 | 0.168 | | 0.01 | 0.7 | 0.398 |
| Precentral L | | | | | | | | |
| $BP_{ND}$ | 0.38 | 0.00 | 0.0 | 0.925 | 0.40 | 0.00 | 0.0 | 0.925 |
| T1/PD | | 0.36[b] | 27.3[b] | <0.001[b] | | 0.40[b] | 31.3[b] | <0.001[b] |
| Group | | 0.06[b] | 4.8[b] | 0.033[b] | | 0.04 | 3.7 | 0.061 |
| Group × $BP_{ND}$ | | 0.02 | 1.4 | 0.249 | | 0.02 | 1.4 | 0.246 |
| Group × T1/PD | | 0.00 | 0.2 | 0.650 | | 0.00 | 0.0 | 0.828 |
| MTG L | | | | | | | | |
| $BP_{ND}$ | 0.45 | 0.12[b] | 6.5[b] | 0.014[b] | 0.45 | 0.12[b] | 6.5[b] | 0.014[b] |
| T1/PD | | 0.34[b] | 30.0[b] | <0.001[b] | | 0.35[b] | 31.0[b] | <0.001[b] |
| Group | | 0.03 | 2.6 | 0.116 | | 0.03 | 2.8 | 0.098 |
| Group × $BP_{ND}$ | | 0.01 | 0.5 | 0.471 | | 0.01 | 0.5 | 0.505 |
| Group × T1/PD | | 0.01 | 0.9 | 0.354 | | 0.01 | 0.6 | 0.431 |
| **Gray matter increases in patients compared with controls** | | | | | | | | |
| Angular gyrus L | | | | | | | | |
| $BP_{ND}$ | 0.56 | 0.32[b] | 22.7[b] | <0.001[b] | 0.61 | 0.32[b] | 22.7[b] | <0.001[b] |
| T1/PD | | 0.22[b] | 22.0[b] | <0.001[b] | | 0.28[b] | 34.0[b] | <0.001[b] |
| Group | | 0.06[b] | 6.4[b] | 0.015[b] | | 0.04[b] | 4.6[b] | 0.038[b] |
| Group × $BP_{ND}$ | | 0.00 | 0.0 | 0.899 | | 0.01 | 0.6 | 0.439 |
| Group × T1/PD | | 0.01 | 1.5 | 0.225 | | 0.01 | 0.6 | 0.430 |

*Table Continued*

**Table 3. (continued)**

| | | | | | | | | |
|---|---|---|---|---|---|---|---|---|
| Cuneus R | | | | | | | | |
| $BP_{ND}$ | 0.81 | $0.70^b$ | $114.0^b$ | $<0.001^b$ | 0.87 | $0.70^b$ | $114.0^b$ | $<0.001^b$ |
| T1/PD | | $0.12^b$ | $33.7^b$ | $<0.001^b$ | | $0.17^b$ | $65.6^b$ | $<0.001^b$ |
| Group | | 0.00 | 1.0 | 0.324 | | 0.00 | 1.1 | 0.298 |
| Group $\times$ $BP_{ND}$ | | 0.00 | 0.9 | 0.358 | | 0.01 | 2.0 | 0.160 |
| Group $\times$ T1/PD | | 0.00 | 0.1 | 0.794 | | 0.00 | 0.1 | 0.795 |
| Postcentral gyrus R | | | | | | | | |
| $BP_{ND}$ | 0.40 | $0.22^b$ | $13.6^b$ | $0.001^b$ | 0.47 | $0.22^b$ | $13.6^b$ | $0.001^b$ |
| T1/PD | | $0.18^b$ | $14.6^b$ | $<0.001^b$ | | $0.24^b$ | $20.7^b$ | $<0.001^b$ |
| Group | | $0.05^b$ | $4.5^b$ | $0.039^b$ | | 0.04 | 3.7 | 0.059 |
| Group $\times$ $BP_{ND}$ | | 0.01 | 0.5 | 0.491 | | 0.01 | 0.6 | 0.447 |
| Group $\times$ T1/PD | | 0.01 | 0.4 | 0.531 | | 0.03 | 2.4 | 0.130 |

[a]GMV served as the dependent variable; flumazenil $BP_{ND}$, T1 time (water content) or proton density (PD), group (patients or controls), and the interaction terms served as the explanatory variables in the multiple regression analysis. L, Left; R, right.

[b]Significant with cluster-level correction across the whole brain at $p < 0.05$.

content an additional 22%, 12%, and 18%, respectively. When water content was included first in the regression model, the variance explained by water content increased, indicating that some of the explained variance could not uniquely be ascribed to $GABA_A$ receptor concentration or water content. Because the variance explained by $GABA_A$ receptor concentration and tissue water was largely separable for areas of decreased GMV, this suggests that $GABA_A$ receptor concentration and water content change concomitantly in areas of GMV increase. The results of the regression analysis were very similar when proton density was used instead of T1 relaxation times. The factor "group" had no influence on the relationship between GMV and $GABA_A$ receptor concentration or water content (Table 3).

**Correlation with clinical variables**

GMV in the PCC was negatively correlated with time since diagnosis ($r = -0.51$, $p = 0.004$) and symptom duration ($r = -0.33$, $p = 0.048$), and GMV in the ACC was negatively correlated with time since diagnosis ($r = -0.52$, $p = 0.007$). This means that the longer the patients have had fibromyalgia, the less gray matter patients had. There was also a trend for a negative correlation between GMV in the PCC and depression scores from the Hospital Anxiety and Depression Scale ($r = -0.29$, $p = 0.073$) and the Beck Depression Inventory ($r = -0.27$, $p = 0.091$) (i.e., the higher the score on the depression scales, less GMV was present).

In the regions of increases, GMV in the angular gyrus was positively correlated with current pain level ($r = 0.35$, $p = 0.04$), the anxiety subscale of the Hospital Anxiety and Depression Scale ($r = 0.36$, $p = 0.034$), and the Pain Catastrophizing Scale ($r = 0.36$, $p = 0.035$). This means that the more severe the pain and psychological symptoms, the more gray matter patients had in this region.

**Replication of PET and VBM relationship**

We largely replicated the findings of positive relationships between gray matter density and flumazenil $BP_{ND}$ by Duncan et al. (2013) (Table 4). In addition to validating the VBM and the $BP_{ND}$ measurements in the present study, this shows that positive relationships between GMVs and flumazenil $BP_{NP}$ are preserved in postmenopausal women.

## Discussion

Here, we investigated the histological underpinnings of regional gray matter alterations in chronic pain using multimodal imaging. Gray matter decreases were largely explained by T1 relaxation times, a surrogate measure of water content, and not to any substantial degree by $GABA_A$ receptor concentration. In

contrast, gray matter increases were explained by $GABA_A$ receptor concentration, in addition to T1 relaxation times. To the best of our knowledge, this is the first time that $GABA_A$ receptor concentration and T1 relaxation times were measured and combined to understand the basis of gray matter alterations in chronic pain.

$GABA_A$ is the most widespread inhibitory receptor in the CNS (Nutt and Malizia, 2001), mainly localized on postsynaptic membranes (for review, see Waldvogel and Faull, 2015), and expressed only weakly in non-neuronal tissue (Fraser et al., 1995; Kullmann et al., 2005). The difference in $GABA_A$ receptor concentration between neuronal and non-neuronal tissues forms the basis for using binding of flumazenil, an antagonist at the benzodiazepine binding site of the $GABA_A$ receptor, as a surrogate of neuronal integrity (Heiss et al., 1998) or density (la Fougère et al., 2011). The finding that regional gray matter decreases were not explained by $GABA_A$ receptor concentration likely indicates that neurons are unaffected in those areas. Alternatively, neurodegeneration is present in patients with fibromyalgia but is masked by concomitant upregulation of $GABA_A$ receptors. Changes in tNA concentrations occur almost invariably when neuronal loss or dysfunction is present (Moffett et al., 2013), which was the rationale to include this measure in the present study. Despite showing decreased gray matter, the ACC did not exhibit a decreased tNA/Cr concentration ratio. Thus, compromised neuronal integrity with concomitant $GABA_A$ receptor upregulation appears to be the less likely explanation, at least for the ACC. These findings are in line with decreased prefrontal cortical thickness in a preclinical model of long-term neuropathic pain (Seminowicz et al., 2009) without concomitant changes in neuronal cell density (Millecamps et al., 2010, data published in abstract form) and with reports of the reversibility of gray matter decreases with successful pain therapy (Rodriguez-Raecke et al., 2009). In contrast to the neuronal measures, the surrogate measure of tissue water content partly explained gray matter decreases. T1 relaxation times exhibited positive linear relationships with GMVs, indicating lower water content in areas with reduced gray matter. Because of potential biases in T1 mapping (Stikov et al., 2015), we also analyzed proton-density maps (Mezer et al., 2013), which are less dependent on lipids and macromolecules than T1 times. This analysis yielded very similar results, supporting the interpretation that GMV decreases in patients were related to decreased water content. Dehydration and altered cerebral blood flow are two potential explanations for the observed contribution of water content. Although manipulation of hydration state can influence morphometric measures (Duning et al., 2005; Streitbürger et al.,
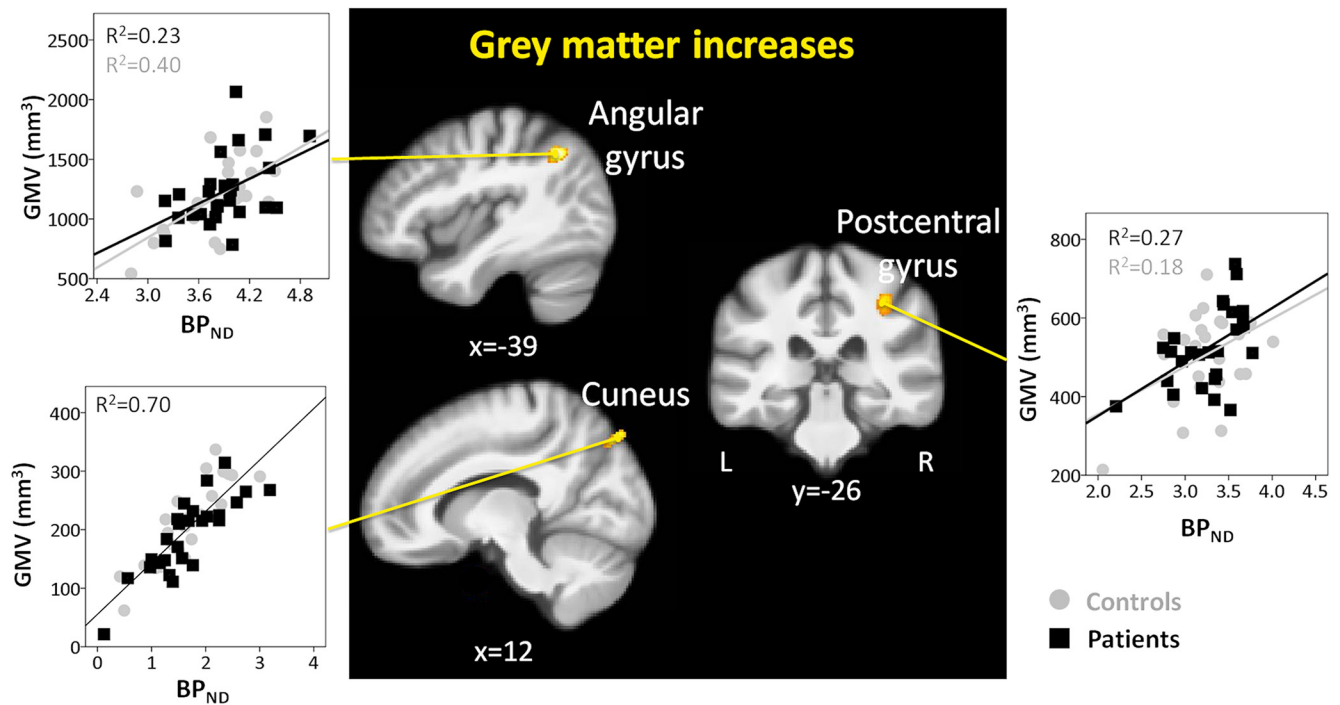
**Figure 4.** GMV increases in patients with fibromyalgia and their relationship with GABA$_A$ receptor concentration. Whole-brain map of gray matter increases in patients compared with controls. Results are presented at a voxelwise threshold of $z > 2.3$ and a cluster-extent threshold of $k > 200$, overlaid on the mean anatomical image of the whole sample ($N = 51$). Scatter plots display GMV (in mm$^3$) against flumazenil BP$_{ND}$ in each cluster. The axial image is displayed in neurological convention. Right, Right hemisphere.

**Table 4. Relationship between gray matter density and flumazenil BP$_{ND}$[a]**

| Region | Gray matter | | | WLS regression | |
|---|---|---|---|---|---|
| | Volume (mm$^3$) | BP$_{ND}$ | GM density | T | p |
| Anterior inferior parietal sulcus | 2406 | 3.08 | 0.45 | 2.98[b] | 0.007[b] |
| Parietal lobule PF | 3385 | 3.94 | 0.61 | 1.68 | 0.107 |
| V3V | 2865 | 3.42 | 0.52 | 1.60 | 0.123 |
| Laterobasal amygdale | 1301 | 2.42 | 0.67 | 2.05 | 0.052 |
| Hippocampus cornu ammonis | 2955 | 2.69 | 0.70 | 2.88[b] | 0.008[b] |
| Hippocampus subiculum L | 2505 | 2.67 | 0.72 | 1.63 | 0.116 |
| Hippocampus subiculum R | 2509 | 2.84 | 0.69 | 1.81 | 0.084 |

[a]Relationship between gray matter density and flumazenil BP$_{ND}$ in regions showing a significant relationship in the Duncan et al. (2013) study. This table replicates the weighted least square (WLS) regression analysis done in Duncan et al. (2013) to investigate the relationship between gray matter density and flumazenil BP$_{ND}$ in our healthy control group ($N = 25$), in regions from the Jülich histological atlas.

[b]Significant with cluster-level correction across the whole brain at $p < 0.05$.

2012), it seems unlikely that differences in hydration status explain the finding of gray matter decreases in patients because there is no evidence of compromised hydration in fibromyalgia, at least to the best of our knowledge. An alternative explanation is reduced cerebral blood flow (Franklin et al., 2013), which might lead to decreased tissue water content by reduced extravasation. Indeed, reduced blood flow has been described in the thalamus in several chronic pain conditions, including fibromyalgia (for review, see Williams and Gracely, 2006). Interestingly, the PCC, which consistently shows decreased gray matter in chronic pain (Smallwood et al., 2013), is part of the default mode network and has a very high metabolic rate at rest (Cavanna and Trimble, 2006), making it perhaps particularly vulnerable to altered cerebral perfusion.

The regions showing gray matter decreases are consistent with previous reports in fibromyalgia (Kuchinad et al., 2007; Luerding et al., 2008; Lutz et al., 2008; Burgmer et al., 2009; Wood et al., 2009; Puri et al., 2010; Robinson et al., 2011; Ceko et al., 2013; Diaz-Piedra et al., 2016) and other chronic pain conditions (Smallwood et al., 2013). In particular, bilateral insula and ACC

are key pain processing regions and the specific subregions found here receive ascending nociceptive input (Dum et al., 2009). The statistically most robust GMV decreases were observed in the PCC and the precuneus, which negatively correlated with disease duration and time since diagnosis: the longer patients had fibromyalgia, the smaller the GMVs. This replicates previous findings in fibromyalgia patients (Kuchinad et al., 2007; Ceko et al., 2013). It also speaks against the group difference being a false-positive finding, which is important because the PCC was recently identified as a "hotspot" of false positives in human brain imaging studies (Eklund et al., 2016). PCC, precuneus, and MPFC, also exhibiting decreased GMV in the patients, are part of the default mode network (Raichle et al., 2001), suggested to be disrupted in chronic pain (Baliki et al., 2008). We further observed decreased gray matter in the precentral gyrus, which is interesting because sensorimotor regions have been found to be key for the classification of chronic pain disorders based on morphometric measures (Labus et al., 2015).

In contrast to areas with decreased gray matter, the variance in regions with increased GMVs was partly explained by GABA$_A$

receptor concentration in addition to T1 relaxation times. Increased flumazenil binding could be due to increased neuronal expression of GABA$_A$ receptors or increases in the amount of neuronal matter. Increased expression of GABA$_A$ receptors has been shown in the spinal cord of rats with neuropathic pain (Lorenzo et al., 2013, data published in abstract form) and decreased supraspinal GABA concentration has been reported in fibromyalgia (Foerster et al., 2012), perhaps leading to compensatory receptor increase. Interestingly, supraspinal GABA$_A$ receptor activation in rats decreases nociceptive thresholds and produces hyperalgesia (Tatsuo et al., 1999), two typical findings in fibromyalgia. Nevertheless, increased GABA$_A$-receptor concentration is not sufficient to explain the finding of increased GMVs. These might be related to inflammatory edema, which could be reflected in the relationship of GMVs with T1 times, or to increases in the amount of neuronal matter, reflected in the relationship of GMV to GABA$_A$ receptor concentration. Candidate cellular mechanisms for increased neuronal matter are increases in the number of neurons or in the size and/or number of dendrites and synapses. An increased number of neurons seems unlikely considering we investigated postmenopausal women. In contrast, remodeling of synapses and dendrites is a well-known phenomenon with increased usage or training (Lerch et al., 2011; Zatorre et al., 2012) also in older age (Bloss et al., 2011). A preclinical model of neuropathic pain showed more dendritic branching and increased spine density in the MPFC (Metz et al., 2009), indicating that neuronal matter is perhaps "induced" by ongoing nociceptive input. GMV increases in the current study concerned brain areas where visual and sensorimotor information converge: the angular gyrus, the cuneus, and the postcentral gyrus are involved in attention to the body and visuomotor coordination (Prado et al., 2005; Macaluso and Maravita, 2010). Thus, increased gray matter in these regions might reflect patients allocating increased attentional resources to nociceptive and other unpleasant sensory stimuli (Schweinhardt et al., 2007). The finding that larger GMVs in the angular gyrus in patients were associated with higher pain levels, the cardinal symptom of fibromyalgia, as well as higher anxiety and higher catastrophic thinking in relation to pain, supports this interpretation.

### Limitations

Although state of the art, the measures used here are indirect measures of the histological underpinnings of gray matter changes. Therefore, their interpretation is not unambiguous. For example, it is known that axon size can bias T1 measurements (Harkins et al., 2016). Also, T1-weighted MR images are based on T1 relaxation times; therefore, these two measures are not strictly independent. Last, flumazenil binding has been used as a marker of neuronal integrity (Heiss et al., 2001) but did not correlate with NAA, a measure of neuronal viability, which emphasizes that flumazenil binding and NAA index different phenomena, with flumazenil binding being representative of neuronal density or of the availability of GABA$_A$ receptors and NAA of neuronal health.

### Outlook and conclusions

Other chronic pain conditions show gray matter alterations in similar brain regions as fibromyalgia (Smallwood et al., 2013), and it will be interesting to establish whether the histological underpinnings are similar to or different from the ones we describe here. Given the observation that gray matter decreases resolve with pain reduction in osteoarthritis (Rodriguez-Raecke et al., 2009), low back pain (Seminowicz et al., 2013), and posttraumatic headache (Obermann et al., 2009), it appears that neu-

rodegeneration does not play a role in these conditions. The present study forms a basis for future work investigating specific hypotheses regarding gray matter alterations in chronic pain, including the relationship to cerebral perfusion or neuroinflammation. Also, animal models of chronic pain conditions will be helpful to better characterize cerebral alterations induced by long-term nociceptive input. Because chronic pain constitutes a major health problem (Mansfield et al., 2016), understanding its neurobiology is crucial. This study provides an important step toward this goal by identifying several potential mechanisms underlying gray matter alterations and indicating that cerebral neurodegeneration is unlikely to play a major role in fibromyalgia. This is in contrast to diseases with established neurodegeneration and therefore indicates that different mechanisms can underlie regional gray matter alterations, as measured with structural MRI, in different clinical conditions.

## References

Anderson BJ (2011) Plasticity of gray matter volume: the cellular and synaptic plasticity that underlies volumetric change. Dev Psychobiol 53:456–465. CrossRef Medline

Ashburner J, Friston KJ (2000) Voxel-based morphometry: the methods. Neuroimage 11:805–821. CrossRef Medline

Baliki MN, Geha PY, Apkarian AV, Chialvo DR (2008) Beyond feeling: chronic pain hurts the brain, disrupting the default-mode network dynamics. J Neurosci 28:1398–1403. CrossRef Medline

Beck AT, Ward CH, Mendelson M, Mock J, Erbaugh J (1961) An inventory for measuring depression. Arch Gen Psychiatry 4:561–571. CrossRef Medline

Bennett R (2005) The Fibromyalgia Impact Questionnaire (FIQ): a review of its development, current version, operating characteristics and uses. Clin Exp Rheumatol 23:S154–S162. Medline

Bloss EB, Janssen WG, Ohm DT, Yuk FJ, Wadsworth S, Saardi KM, McEwen BS, Morrison JH (2011) Evidence for reduced experience-dependent dendritic spine plasticity in the aging prefrontal cortex. J Neurosci 31:7831–7839. CrossRef Medline

Bobinski M, de Leon MJ, Wegiel J, Desanti S, Convit A, Saint Louis LA, Rusinek H, Wisniewski HM (2000) The histological validation of post mortem magnetic resonance imaging-determined hippocampal volume in Alzheimer's disease. Neuroscience 95:721–725. CrossRef Medline

Bottomley PA (1984) Selective volume method for performing localized NMR spectroscopy. US patent. Medline.

Burgmer M, Gaubitz M, Konrad C, Wrenger M, Hilgart S, Heuft G, Pfleiderer B (2009) Decreased gray matter volumes in the cingulo-frontal cortex and the amygdala in patients with fibromyalgia. Psychosom Med 71:566–573. CrossRef Medline

Bushnell MC, Ceko M, Low LA (2013) Cognitive and emotional control of pain and its disruption in chronic pain. Nat Rev Neurosci 14:502–511. CrossRef Medline

Cavanna AE, Trimble MR (2006) The precuneus: a review of its functional anatomy and behavioural correlates. Brain 129:564–583. CrossRef Medline

Ceko M, Bushnell MC, Fitzcharles MA, Schweinhardt P (2013) Fibromyalgia interacts with age to change the brain. Neuroimage Clin 3:249–260. CrossRef Medline

Cheng HL, Stikov N, Ghugre NR, Wright GA (2012) Practical medical applications of quantitative MR relaxometry. J Magn Reson Imaging 36:805–824. CrossRef Medline

Craig CL, Marshall AL, Sjöström M, Bauman AE, Booth ML, Ainsworth BE, Pratt M, Ekelund U, Yngve A, Sallis JF, Oja P (2003) International Physical Activity Questionnaire: 12-country reliability and validity. Med Sci Sports Exerc 35:1381–1395. CrossRef Medline

Davis KD, Moayedi M (2013) Central mechanisms of pain revealed through functional and structural MRI. J Neuroimmune Pharmacol 8:518–534. CrossRef Medline

Deoni SC, Peters TM, Rutt BK (2005) High-resolution T1 and T2 mapping of the brain in a clinically acceptable time with DESPOT1 and DESPOT2. Magn Reson Med 53:237–241. CrossRef Medline

Diaz-Piedra C, Guzman MA, Buela-Casal G, Catena A (2016) The impact of

fibromyalgia symptoms on brain morphometry. Brain Imaging Behav 10:1184–1197. CrossRef Medline

Draganski B, Ashburner J, Hutton C, Kherif F, Frackowiak RS, Helms G, Weiskopf N (2011) Regional specificity of MRI contrast parameter changes in normal ageing revealed by voxel-based quantification (VBQ). Neuroimage 55:1423–1434. CrossRef Medline

Dum RP, Levinthal DJ, Strick PL (2009) The spinothalamic system targets motor and sensory areas in the cerebral cortex of monkeys. J Neurosci 29:14223–14235. CrossRef Medline

Duncan NW, Gravel P, Wiebking C, Reader AJ, Northoff G (2013) Grey matter density and GABAA binding potential show a positive linear relationship across cortical regions. Neuroscience 235:226–231. CrossRef

Duning T, Kloska S, Steinsträter O, Kugel H, Heindel W, Knecht S (2005) Dehydration confounds the assessment of brain atrophy. Neurology 64: 548–550. CrossRef Medline

Duyckaerts C, Delatour B, Potier MC (2009) Classification and basic pathology of Alzheimer disease. Acta Neuropathol 118:5–36. CrossRef Medline

Eickhoff SB, Heim S, Zilles K, Amunts K (2006) Testing anatomically specified hypotheses in functional imaging using cytoarchitectonic maps. Neuroimage 32:570–582. CrossRef Medline

Eickhoff SB, Paus T, Caspers S, Grosbras MH, Evans AC, Zilles K, Amunts K (2007) Assignment of functional activations to probabilistic cytoarchitectonic areas revisited. Neuroimage 36:511–521. CrossRef Medline

Eklund A, Nichols TE, Knutsson H (2016) Cluster failure: why fMRI inferences for spatial extent have inflated false-positive rates. Proc Natl Acad Sci U S A 113:7900–7905. CrossRef Medline

Fan J, McCandliss BD, Sommer T, Raz A, Posner MI (2002) Testing the efficiency and independence of attentional networks. J Cogn Neurosci 14:340–347. CrossRef Medline

Fatouros PP, Marmarou A, Kraft KA, Inao S, Schwarz FP (1991) In vivo brain water determination by T1 measurements: effect of total water content, hydration fraction, and field strength. Magn Reson Med 17:402–413. CrossRef Medline

Fitzcharles MA, Ste-Marie PA, Goldenberg DL, Pereira JX, Abbey S, Choinière M, Ko G, Moulin DE, Panopalis P, Proulx J, Shir Y (2013) 2012 Canadian guidelines for the diagnosis and management of fibromyalgia syndrome: executive summary. Pain Res Manag 18:119–126. CrossRef Medline

Foerster BR, Petrou M, Edden RA, Sundgren PC, Schmidt-Wilcke T, Lowe SE, Harte SE, Clauw DJ, Harris RE (2012) Reduced insular γ-aminobutyric acid in fibromyalgia. Arthritis Rheum 64:579–583. CrossRef Medline

Franklin TR, Wang Z, Shin J, Jagannathan K, Suh JJ, Detre JA, O'Brien CP, Childress AR (2013) A VBM study demonstrating "apparent" effects of a single dose of medication on T1-weighted MRIs. Brain Struct Funct 218:97–104. CrossRef Medline

Fraser DD, Duffy S, Angelides KJ, Perez-Velazquez JL, Kettenmann H, MacVicar BA (1995) GABAA/benzodiazepine receptors in acutely isolated hippocampal astrocytes. J Neurosci 15:2720–2732. Medline

Funck T, Paquette C, Evans A, Thiel A (2014) Surface-based partial-volume correction for high-resolution PET. Neuroimage 102:674–687. CrossRef Medline

Gelman N, Ewing JR, Gorell JM, Spickler EM, Solomon EG (2001) Interregional variation of longitudinal relaxation rates in human brain at 3.0 T: relation to estimated iron and water contents. Magn Reson Med 45:71–79. CrossRef Medline

Hammers A, Koepp MJ, Richardson MP, Hurlemann R, Brooks DJ, Duncan JS (2003) Grey and white matter flumazenil binding in neocortical epilepsy with normal MRI: a PET study of 44 patients. Brain 126:1300–1318. CrossRef Medline

Harkins KD, Xu J, Dula AN, Li K, Valentine WM, Gochberg DF, Gore JC, Does MD (2016) The microstructural correlates of T1 in white matter. Magn Reson Med 75:1341–1345. CrossRef Medline

Heiss WD, Grond M, Thiel A, Ghaemi M, Sobesky J, Rudolf J, Bauer B, Wienhard K (1998) Permanent cortical damage detected by flumazenil positron emission tomography in acute stroke. Stroke 29:454–461. CrossRef Medline

Heiss WD, Kracht LW, Thiel A, Grond M, Pawlik G (2001) Penumbral probability thresholds of cortical flumazenil binding and blood flow predicting tissue outcome in patients with cerebral ischaemia. Brain 124:20–29. CrossRef Medline

Holthoff VA, Koeppe RA, Frey KA, Paradise AH, Kuhl DE (1991) Differentiation of radioligand delivery and binding in the brain: validation of a two-compartment model for [11C]flumazenil. J Cereb Blood Flow Metab 11:745–752. CrossRef Medline

Kuchinad A, Schweinhardt P, Seminowicz DA, Wood PB, Chizh BA, Bushnell MC (2007) Accelerated brain gray matter loss in fibromyalgia patients: premature aging of the brain? J Neurosci 27:4004–4007. CrossRef Medline

Kullmann DM, Ruiz A, Rusakov DM, Scott R, Semyanov A, Walker MC (2005) Presynaptic, extrasynaptic and axonal GABAA receptors in the CNS: where and why? Prog Biophys Mol Biol 87:33–46. CrossRef Medline

Kurth F, Gaser C, Luders E (2015) A 12-step user guide for analyzing voxelwise gray matter asymmetries in statistical parametric mapping (SPM). Nat Protoc 10:293–304. CrossRef Medline

Labus JS, Van Horn JD, Gupta A, Alaverdyan M, Torgerson C, Ashe-McNalley C, Irimia A, Hong JY, Naliboff B, Tillisch K, Mayer EA (2015) Multivariate morphological brain signatures predict patients with chronic abdominal pain from healthy control subjects. Pain 156:1545–1554. CrossRef Medline

la Fougère C, Grant S, Kostikov A, Schirrmacher R, Gravel P, Schipper HM, Reader A, Evans A, Thiel A (2011) Where in-vivo imaging meets cytoarchitectonics: the relationship between cortical thickness and neuronal density measured with high-resolution [18F]flumazenil-PET. Neuroimage 56:951–960. CrossRef Medline

Lerch JP, Yiu AP, Martinez-Canabal A, Pekar T, Bohbot VD, Frankland PW, Henkelman RM, Josselyn SA, Sled JG (2011) Maze training in mice induces MRI-detectable brain shape changes specific to the type of learning. Neuroimage 54:2086–2095. CrossRef Medline

Lorenzo LE, Price T, Pitcher M (2013) Targeting spinal GABAergic mechanisms to develop novel analgesics. Presented at American Pain Society 32nd Annual Scientific Meeting, New Orleans, LA. Symposium 327.

Lorio S, Kherif F, Ruef A, Melie-Garcia L, Frackowiak R, Ashburner J, Helms G, Lutti A, Draganski B (2016) Neurobiological origin of spurious brain morphological changes: a quantitative MRI study. Hum Brain Mapp 37:1801–1815. CrossRef Medline

Luerding R, Weigand T, Bogdahn U, Schmidt-Wilcke T (2008) Working memory performance is correlated with local brain morphology in the medial frontal and anterior cingulate cortex in fibromyalgia patients: structural correlates of pain-cognition interaction. Brain 131:3222–3231. CrossRef Medline

Lutz J, Jäger L, de Quervain D, Krauseneck T, Padberg F, Wichnalek M, Beyer A, Stahl R, Zirngibl B, Morhard D, Reiser M, Schelling G (2008) White and gray matter abnormalities in the brain of patients with fibromyalgia: a diffusion-tensor and volumetric imaging study. Arthritis Rheum 58:3960–3969. CrossRef Medline

Macaluso E, Maravita A (2010) The representation of space near the body through touch and vision. Neuropsychologia 48:782–795. CrossRef Medline

Mansfield KE, Sim J, Jordan JL, Jordan KP (2016) A systematic review and meta-analysis of the prevalence of chronic widespread pain in the general population. Pain 157:55–64. CrossRef Medline

Massaweh G, Schirrmacher E, la Fougère C, Kovacevic M, Wängler C, Jolly D, Gravel P, Reader AJ, Thiel A, Schirrmacher R (2009) Improved work-up procedure for the production of [18] flumazenil and first results of its use with a high-resolution research tomograph in human stroke. Nucl Med Biol 36:721–727. CrossRef Medline

Mease P, Arnold LM, Choy EH, Clauw DJ, Crofford LJ, Glass JM, Martin SA, Morea J, Simon L, Strand CV, Williams DA (2009) Fibromyalgia syndrome module at OMERACT 9: domain construct. J Rheumatol 36:2318–2329. CrossRef Medline

Metz AE, Yau HJ, Centeno MV, Apkarian AV, Martina M (2009) Morphological and functional reorganization of rat medial prefrontal cortex in neuropathic pain. Proc Natl Acad Sci U S A 106:2423–2428. CrossRef Medline

Mezer A, Yeatman JD, Stikov N, Kay KN, Cho NJ, Dougherty RF, Perry ML, Parvizi J, Hua le H, Butts-Pauly K, Wandell BA (2013) Quantifying the local tissue volume and composition in individual brains with magnetic resonance imaging. Nat Med 19:1667–1672. CrossRef Medline

Millecamps M, Seminowicz DA, Laferriere AL, Kocsis P, Coderre TJ, Stone LS, et al. (2010) Histological changes associated with prefrontal cortex atrophy in a rodent model of long term neuropathy. Presented at IASP Conference, Montréal, QC, Canada.

Moffett JR, Namboodiri MA, Cangro CB, Neale JH (1991) Immunohisto-chemical localization of N-acetylaspartate in rat brain. Neuroreport 2:131–134. CrossRef Medline

Moffett JR, Ross B, Arun P, Madhavarao CN, Namboodiri AM (2007) N-Acetylaspartate in the CNS: from neurodiagnostics to neurobiology. Prog Neurobiol 81:89–131. CrossRef Medline

Moffett JR, Ariyannur P, Arun P, Namboodiri AMA (2013) N-Ace-tylaspartate and N-acetylaspartylglutamate. In: Central nervous system health and disease. Amsterdam: Elsevier.

Mueller S, Keeser D, Reiser MF, Teipel S, Meindl T (2012a) Functional and structural MR imaging in neuropsychiatric disorders: 1. Imaging tech-niques and their application in mild cognitive impairment and Alzheimer disease. AJNR Am J Neuroradiol 33:1845–1850. CrossRef Medline

Mueller S, Keeser D, Reiser MF, Teipel S, Meindl T (2012b) Functional and structural MR imaging in neuropsychiatric disorders: 2. Application in schizophrenia and autism. AJNR Am J Neuroradiol 33:2033–2037. CrossRef Medline

Nordahl TE, Salo R, Possin K, Gibson DR, Flynn N, Leamon M, Galloway GP, Pfefferbaum A, Spielman DM, Adalsteinsson E, Sullivan EV (2002) Low N-acetyl-aspartate and high choline in the anterior cingulum of recently abstinent methamphetamine-dependent subjects: a preliminary proton MRS study: magnetic resonance spectroscopy. Psychiatry Res 116:43–52. CrossRef Medline

Nutt DJ, Malizia AL (2001) New insights into the role of the GABA(A)-benzodiazepine receptor in psychiatric disorder. Br J Psychiatry 179:390–396. CrossRef Medline

Obermann M, Nebel K, Schumann C, Holle D, Gizewski ER, Maschke M, Goadsby PJ, Diener HC, Katsarava Z (2009) Gray matter changes related to chronic posttraumatic headache. Neurology 73:978–983. CrossRef Medline

Prado J, Clavagnier S, Otzenberger H, Scheiber C, Kennedy H, Perenin MT (2005) Two cortical systems for reaching in central and peripheral vision. Neuron 48:849–858. CrossRef Medline

Provencher SW (1993) Estimation of metabolite concentrations from local-ized in vivo proton NMR spectra. Magn Reson Med 30:672–679. CrossRef Medline

Puri BK, Agour M, Gunatilake KD, Fernando KA, Gurusinghe AI, Treasaden IH (2010) Reduction in left supplementary motor area grey matter in adult female fibromyalgia sufferers with marked fatigue and without af-fective disorder: a pilot controlled 3-T magnetic resonance imaging voxel-based morphometry study. J Int Med Res 38:1468–1472. CrossRef Medline

Raichle ME, MacLeod AM, Snyder AZ, Powers WJ, Gusnard DA, Shulman GL (2001) A default mode of brain function. Proc Natl Acad Sci U S A 98:676–682. CrossRef Medline

Robinson ME, Craggs JG, Price DD, Perlstein WM, Staud R (2011) Gray matter volumes of pain-related brain areas are decreased in fibromyalgia syndrome. J Pain 12:436–443. CrossRef Medline

Rodriguez-Raecke R, Niemeier A, Ihle K, Ruether W, May A (2009) Brain gray matter decrease in chronic pain is the consequence and not the cause of pain. J Neurosci 29:13746–13750. CrossRef Medline

Schweinhardt P, Sauro KM, Bushnell MC (2008) Fibromyalgia: a disorder of the brain? Neuroscientist 14:415–421. CrossRef Medline

Schweinhardt P, Kuchinad A, Pukall CF, Bushnell MC (2008) Increased gray matter density in young women with chronic vulvar pain. Pain 140:411–419. CrossRef Medline

Seminowicz DA, Laferriere AL, Millecamps M, Yu JS, Coderre TJ, Bushnell MC (2009) MRI structural brain changes associated with sensory and emotional function in a rat model of long-term neuropathic pain. Neu-roimage 47:1007–1014. CrossRef Medline

Seminowicz DA, Shpaner M, Keaser ML, Krauthamer GM, Mantegna J, Dumas JA, Newhouse PA, Filippi CG, Keefe FJ, Naylor MR (2013) Cognitive-behavioral therapy increases prefrontal cortex gray matter in patients with chronic pain. J Pain 14:1573–1584. CrossRef Medline

Sette G, Baron JC, Young AR, Miyazawa H, Tillet I (1993) In vivo mapping of brain benzodiazepine receptor changes by positron emission tomogra-phy after focal ischemia in the anesthetized baboon. Stroke 24:2046–2057; discussion 2057–2058. CrossRef Medline

Smallwood RF, Laird AR, Ramage AE, Parkinson AL, Lewis J, Clauw DJ, Williams DA, Schmidt-Wilcke T, Farrell MJ, Eickhoff SB, Robin DA (2013) Structural brain anomalies and chronic pain: a quantitative meta-analysis of gray matter volume. J Pain 14:663–675. CrossRef Medline

Staud R (2006) Biology and therapy of fibromyalgia: pain in fibromyalgia syndrome. Arthritis Res Ther 8:208. CrossRef Medline

Stikov N, Campbell JS, Stroh T, Lavelée M, Frey S, Novek J, Nuara S, Ho MK, Bedell BJ, Dougherty RF, Leppert IR, Boudreau M, Narayanan S, Duval T, Cohen-Adad J, Picard PA, Gasecka A, Côté D, Pike GB (2015) In vivo histology of the myelin g-ratio with magnetic resonance imaging. Neuro-image 118:397–405. CrossRef Medline

Streitbürger DP, Möller HE, Tittgemeyer M, Hund-Georgiadis M, Schroeter ML, Mueller K (2012) Investigating structural brain changes of dehy-dration using voxel-based morphometry. PLoS One 7:e44195. CrossRef Medline

Stuss DT, Stethem LL, Pelchat G (1988) Three tests of attention and rapid information processing: an extension. Clin Neuropsychol 2:246–250. CrossRef

Sullivan MJL, Bishop SR, Pivik J (1995) The pain catastrophizing scale: de-velopment and validation. Psychol Assess 7:524–532. CrossRef

Tatsuo MA, Salgado JV, Yokoro CM, Duarte ID, Francischi JN (1999) Midazolam-induced hyperalgesia in rats: modulation via GABA(A) re-ceptors at supraspinal level. Eur J Pharmacol 370:9–15. CrossRef Medline

Waldvogel HJ, Faull RL (2015) The diversity of GABAA receptor subunit distribution in the normal and Huntington's disease human brain. Am-sterdam: Elsevier.

Williams DA, Gracely RH (2006) Biology and therapy of fibromyalgia: functional magnetic resonance imaging findings in fibromyalgia. Arthri-tis Res Ther 8:224. CrossRef Medline

Wood PB, Glabus MF, Simpson R, Patterson JC 2nd (2009) Changes in gray matter density in fibromyalgia: correlation with dopamine metabolism. J Pain 10:609–618. CrossRef Medline

Worsley KJ, Andermann M, Koulis T, MacDonald D, Evans AC (1999) De-tecting changes in nonisotropic images. Hum Brain Mapp 8:98–101. CrossRef Medline

Worsley KJ, Taylor JE, Tomaiuolo F, Lerch J (2004) Unified univariate and multivariate random field theory. Neuroimage 23 [Suppl 1]:S189–S195. CrossRef Medline

Yarnykh VL (2007) Actual flip-angle imaging in the pulsed steady state: a method for rapid three-dimensional mapping of the transmitted radio-frequency field. Magn Reson Med 57:192–200. Medline

Zatorre RJ, Fields RD, Johansen-Berg H (2012) Plasticity in gray and white: neuroimaging changes in brain structure during learning. Nat Neurosci 15:528–536. CrossRef Medline

Zigmond AS, Snaith RP (1983) The hospital anxiety and depression scale. Acta Psychiatr Scand 67:361–370. CrossRef Medline